OVERVIEW OF THE APT HIGH-ENERGY BEAM TRANSPORT AND BEAM EXPANDERS

R. E. Shafer, B. Blind, E. R. Gray, J. D. Gilpatrick, D. Barlow, and G. P. Lawrence.

Abstract

The APT high energy beam transport (HEBT) and beam expanders convey the 1700-MeV, 100-mA cw proton beam from the linac to the tritium target/blanket assembly, or a tuning beam stop. The HEBT includes extensive beam diagnostics, collimators, and beam jitter correction, to monitor and control the 170-MW beam prior to expansion. A zero-degree beamline conveys the beam to the beam stop, and an achromatic beand conveys the beam to the tritium production target. Nonlinear beam expanders make use of higher-order multipole magnets and dithering dipoles to expand the beam to a uniform-density, 16-cm wide by 160-cm high rectangular profile on the tritium-production target. The overall optics design will be reviewed, and beam simulations will be presented.

1 INTRODUCTION

The Accelerator for Production of Tritium (APT) is a 1700-MeV, 100-mA cw proton accelerator designed for the production of tritium in a target/blanket assembly via the reaction ^{3}He(n,p)T [1]. The beam from the 700-MHz superconducting (SC) rf linac [2] is transported to either a 4-MW low-duty-factor beam stop, or the tritium-production target by means of the high energy beam transport (HEBT), the switchyard and bend, and beam expanders.

The overall beamline layout is shown in Fig. 1. The approximate beamline length is 250 m from the linac to the beam stop, and 280 m from the linac to the tritium production target.

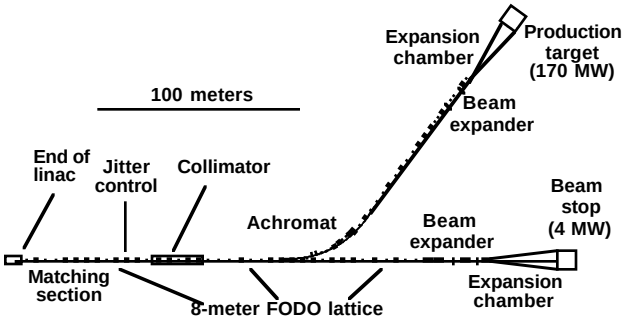

Fig. 1. The overall layout of the APT beam delivery system.

The purpose of the beam delivery system is to transport the beam to either of the end stations and expand it, to reduce the beam power density to acceptable levels. The HEBT includes beam diagnostics to characterize and monitor the beam, a system to correct beam position and angle jitter, and a collimator to intercept beam halo. The switchyard, which includes a 53.13°, 5-FODO-period achromat, directs the beam to either the beam stop or the tritium-production target. Finally, the beam expanders transform the beam to a 16-cm-wide by 160-cm-high uniform density distribution at the target windows. Each of these systems is described in more detail below.

2 HEBT AND EXPANDER LAYOUT

2.1 High Energy Beam Transport

The HEBT consists of an 8-meter-period FODO lattice, with a 72° zero-current phase advance per period. This 8-meter periodicity is maintained throughout the HEBT and switchyard to both end stations. The initial HEBT aperture is 16-cm diameter, to match the aperture in the superconducting (SC) linac [2]. The first 29 m is an adiabatic match from the SC linac focusing lattice. This FODO lattice also includes beam diagnostics to characterize and monitor beam energy, beam current, beam profiles, and a beam jitter control system to remove any residual transverse beam jitter and steering errors not corrected by the beam steering control system in the linac. The beam diagnostics for characterizing the linac is described elsewhere [3].

This HEBT section is followed by a 20-m-long adjustable-aperture collimator system to remove any excessive beam halo that might result from mismatches, beam turn-on transients, or component failure in the linac. The collimator is specifically designed to absorb up to about 1 kW of beam continuously, or individual pulses of 5 kJ, corresponding to about 30 μsec of full-power beam. This unit is heavily shielded, and is specifically designed to allow remote maintenance.

The remainder of the HEBT is a continuation of the same FODO lattice, but with the aperture reduced to 8-cm-diameter.

The nominal rms beam radius in the HEBT is about 1 mm, corresponding to a normalized rms emittance of 0.2 π-mm-mrad. The nominal aperture to beam-size ratio is 70:1 in the 16-cm dia. section, and 35:1 in the 8-cm dia. section.

2.2 Switchyard and Bend

The switchyard includes a 40-m section of the 8-m FODO lattice, a FODO cell with a dipole insertion for directing the beam to either the target or the beam stop, and a 5-FODO period, 360°-zero current phase advance, 53.13° achromat. The dipoles are placed immediately downstream of D-quads to minimize the dispersion in the achromat to about 2.6 cm per % Δp/p. Each dipole is about 1.3-m long, with a field of 1.2 T, and has a bend angle of 10.63°. Each quadrupole has a GL product of about 2.5 T. The beam aperture of the dipoles is 11 cm horizontally, and 7.3 cm vertically, while the beam aperture of the achromat quadrupoles is 9 cm. The energy acceptance of the achromat is ± 20 MeV.

The high-dispersion areas of the achromat will be used for both momentum collimation and for measurement of beam energy and energy spread. Beam

0-7803-4376-X/98/$10.00

energy is also measured in the HEBT using time of flight diagnostics. Momentum collimators will have adjustable apertures to intercept off-momentum beam halo, and off-momentum beams that may result from linac klystron trips. At the high dispersion points, the 2-MeV expected energy spread contributes about 2-mm to the horizontal beam size, compared to the 2-mm width in zero-dispersion areas. Thus both energy spread and energy changes can be observed in these high dispersion regions.

If needed, a second achromat can be inserted in the FODO lattice 40-m upstream of the first one.

2.3 Beam expander

The purpose of the beam expander is to expand the beam from its nominal 2-mm width to a uniform-density, 16-cm wide by 160-cm high image on the target. The nonlinear beam expander optics includes about 50-m of magnetic optics that sequentially folds the vertical and horizontal tails of the nearly Gaussian beam profile back onto the core, in order to achieve a nearly rectangular expanded-beam having a unifirm profile with a 10:1 aspect ratio [4]. The beam expander optics, shown in Fig. 2, include a 4-quadrupole matching section, a nonlinear magnet to fold the beam in the y-y´ phase space, a two-quadrupole intermediate lens, a second nonlinear magnet to fold the beam in the x-x´ phase space, two dithering dipoles to shake the expanded beam ± 1 cm horizontally and ± 2 cm vertically, and a final quadrupole-doublet objective lens to focus the beam through two neutron backshine shields in the beam expansion chamber.

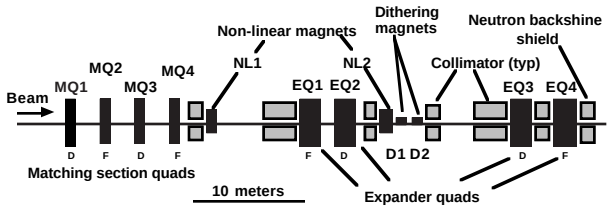

Fig. 2. Beam expander optics.

The beam folding in each plane is carried out in two stages, as illustrated in Fig. 3. First, the nonlinear magnetic fields, including octupole and higher-order terms, fold the beam phase-ellipse in y´ (or x´) space. Then, when the beam drifts in a long field-free region, the beam ellipse shears in y (or x) space, causing the tails in the transverse profile to fold back onto the core of the beam. This folding is done sequentially in the y-y´ and the x-x´ phase spaces.

Two nonlinear (multipole) magnets suitable for beam folding at 800 MeV have been built, and are now being tested at LANSCE in a prototype nonlinear beam expander [5].

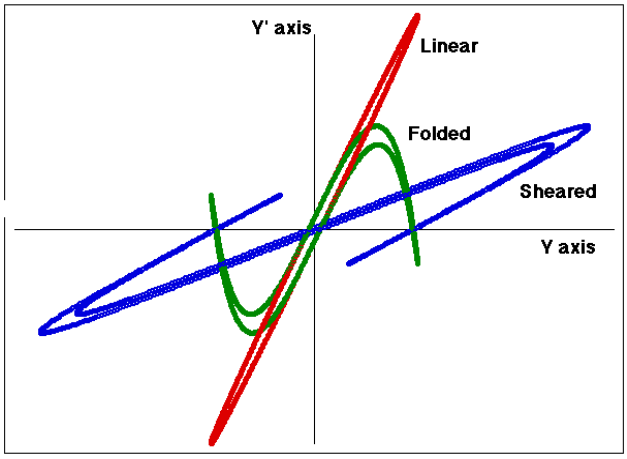

Fig. 3. The folding process for the nonlinear magnets.

Because of the concern about beam losses in the small apertures of the nonlinear expander, an alternate expansion scheme using rastering is being studied. This system is based on a high frequency triangle current-waveform modulator using IGBTs (insulated gate bipolar transistors) with ferrite dipole deflector magnets [6]. This triangular current waveform produces a uniform beam power density on the target. Four independently-powered deflectors, each about 40-cm long, are used in each plane to raster the beam at about 500 Hz vertically and 575 Hz horizontally. This beam-expansion concept has a much larger beam aperture than the nonlinear folding concept, and potentially improved control of the beam distribuion on the target (independent of the input beam), but has the additional risk of thermal fatigue in the target, and the possibility of target damage in the case of raster system failure. These issues are being addressed in the study.

2.4 Beam expansion chamber

Fig. 4 shows the 30-m long beam expansion chamber. In order to limit the backstreaming neutron flux from the target, the expansion chamber includes two neutron backshine shields. These shields are placed at the vertical waist in the expanding beam, about 0.5 m downstream of the last quadrupole, and at the horizontal waist, about 11-m downstream of the last quadrupole. These neutron shields are about 1.5-m-thick iron shields, with a 2-cm high by 15-cm wide contoured slit at the vertical waist, and a 3-cm wide by 80-cm high contoured slit at the horizontal waist. Their upstream side will be covered with a boron-loaded material to absorb low-energy neutrons. The expected backstreaming neutron flux inside the beam expander optics is about 3 x 10^9 n/cm^2/s, and the annual neutron fluence is of the order of 1 x 10^{17} neutrons/cm^2, because the neutron shields together limit the view of the target from the beam expander to about 2% of the target frontal surface area.

The beam expansion chamber includes extensive multiwire beam diagnostics (secondary emission and resistance wires) to determine and monitor the expanded beam profile. These beam diagnostics systems, described elsewhere [3], are inserted through either of two beam diagnostics towers, shown in Fig. 4.

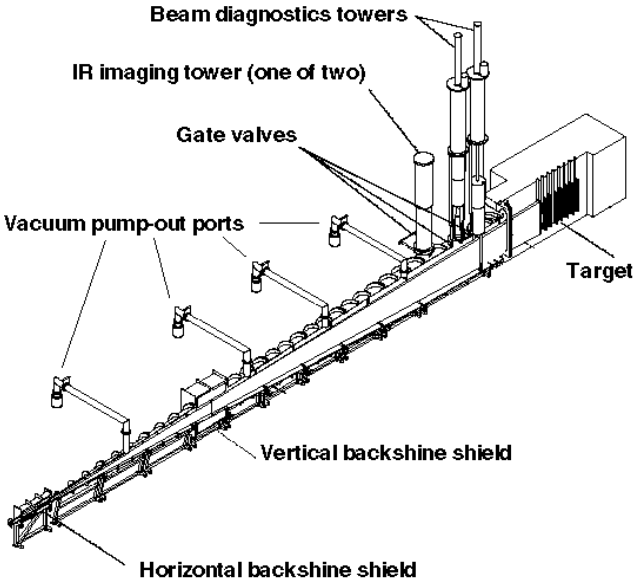

Fig. 4. 30-m long beam expansion chamber.

3 BEAM SIMULATIONS

Beam simulations using space-charge codes (PARMILA and TRACE-3D) show that the SC linac beam is easily matched into the 8-m period FODO lattice from the SC linac wihout any indication of space-charge effects in the transverse planes. The aperture to rms beam size ratio is about 70:1 in the 16 cm diameter HEBT, and 35:1 in the 8-cm diameter section. The longitudinal bunch length of the individual microbunches grows slightly in the HEBT as expected, but this is inconsequential. In addition, the beam simulations through the achromat show no space-charge effects. The maximum dispersion in the achromat is about 2.6 cm per % $\Delta p/p$. With a total energy spread of 2 MeV, the beam width increases by about 2 mm in the achromat. The residual dispersion after the achromat is near zero, and the beam shows no residual effects of the 53.13° bend.

In the beam expander, the 4-quadrupole matching section focuses the beam into the first nonlinear magnet with a horizontal beam waist, and into the second with a vertical waist. The folded beam then expands in both planes to the final quadrupole doublet.

End-to-end particle-tracking simulations, from the RFQ to the tritium-production target, are being used to evaluate the beam-expander design. These simulations include up to 100,000 particles, and include effects such as rf phase and amplitude errors, loss of one klystron, quadrupole field and alignment errors, etc. The simulations indicate that roughly 1 particle in 100,000 either may hit collimators shielding the nonlinear-magnet coils, or may be deflected by a nonlinear magnet into downstream collimators. This is equivalent to 1000 to 2000 watts of beam loss, and may lead to radiation damage and premature beamline-component failure (magnets and beam diagnostics), and indicates the need for remote maintenance capability. The beam expander physics model used in the simulations is being improved to better ascertain the expected beam loss, and design work is going on to increase the physical aperture of the nonlinear magnets [7].

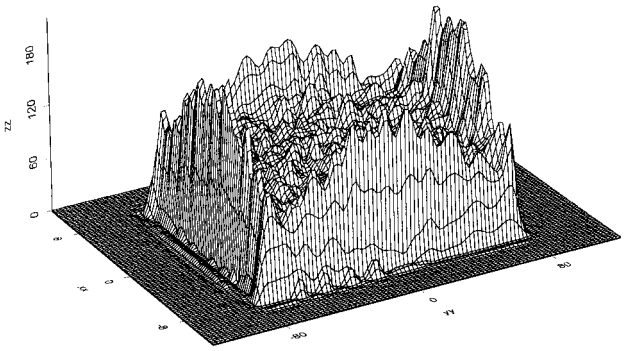

Fig. 5. Isometric plot of simulated particle distribution on target. The horizontal width is 16 cm, and the vertical height is 160 cm.

4 CONCLUSION

The conceptual design of the high energy beam transport to the beam expanders is nearly complete, and meets all the necessary requirements for the APT project. Design of the nonlinear beam expanders is still in progress, with the major effort being to improving the models used in the beam simulations, simulating a wide variety of off-normal linac operating conditions, and increasing the expander magnet apertures. A parallel effort is examining the alternate expansion scheme based on beam rastering.

5 REFERENCES

[1] P. W. Lisowski, “The Accelerator Production of Tritium (APT) Project”, these proceedings.

[2] G. P. Lawrence and T. Wangler, “Integrated Normal/Superconducting Linac Design for APT”, these proceedings.

[3] J. D. Gilpatrick et al., “LEDA and APT Beam Diagnostics Instrumentation,” these proceedings.

[4] B. Blind, “Production of Uniform and Well-Confined Beams by Nonlinear Optics,” Nucl. Inst. and Meth., Vol B56/57, pages 1099-1102 (1991).

[5] D. Barlow et al., “Magnetic Design and Measurement of Nonlinear Multipole Magnets for the APT Beam Expander System,” these proceedings.

[6] C. R. Rose and R. E. Shafer, “A 200-A, 500-Hz Triangle Current-Wave Modulator and Magnet for Particle Beam Rastering,” these proceedings.

[7] A. J. Jason, B. Blind, and K. Halbach, “Beam Expansion with Specified Final Distribution,” these proceedings.